Interactions of Water Vapor with Oxides at Elevated Temperatures

Nathan Jacobson
NASA Glenn Research Center
Cleveland, OH 44135

Elizabeth Opila
Cleveland State University/NASA Glenn Research Center
Cleveland, OH 44135

Evan Copland
Case Western Reserve University/NASA Glenn Research Center
Cleveland, OH 44135

Dwight Myers
East Central University
Ada, OK 74820

Abstract

Many volatile metal hydroxides form by reaction of the corresponding metal oxide with water vapor. These reactions are important in a number of high temperature corrosion processes. Experimental methods for studying the thermodynamics of metal hydroxides include: gas leak Knudsen cell mass spectrometry, free jet sampling mass spectrometry, transpiration and hydrogen-oxygen flame studies. The available experimental information is reviewed and the most stable metal hydroxide species are correlated with position in the periodic table. Current studies in our laboratory on the Si-O-H system are discussed.

Introduction—Importance of Volatile Hydroxides in Corrosion

A number of elements form volatile hydroxides of the general formula $M(OH)_n$ or oxy-hydroxides of the general formula $MO_p(OH)_q$. These form by either of two reaction routes [1,2]:

$$\text{Hydroxides (s,l)} = \text{Hydroxide (g)} \qquad (1)$$

$$\text{e.g. } KOH(s) = KOH(g) \qquad (1a)$$

Oxide (s,l) + H$_2$O(g) = Hydroxide (g) or Oxy-hydroxide (g)   (2)

  e.g. BeO(s) + H$_2$O(g) = Be(OH)$_2$(g)   (2a)

  e.g. MoO$_3$(s) + H$_2$O(g) = MoO$_2$(OH)$_2$(g)   (2b)
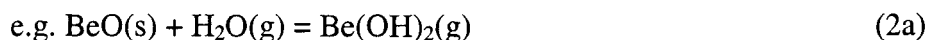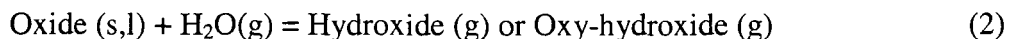
Here we shall focus on reactions of the second type, which are important in a number of high-temperature corrosion processes. Many high temperature corrosion processes occur in combustion environments. Generally hydrocarbon fuel combustion atmospheres contain ~10% water vapor [3]. For 1 bar total pressure, 0.1 bar water vapor is formed; for higher pressure combustion processes an even higher pressure of water vapor is formed. Further, combustion processes in a heat engine typically involve rapidly flowing gases. Together with reaction route (2) this leads to a substantial removal of material.

There are numerous examples of metal hydroxide formation in corrosion processes. Zaplatynsky [4] has exposed a number of commercial Ni-base alloys to air at 1200° C. Depending on the alloy, he observed volatilization of tungsten, molybdenum, niobium, manganese, and chromium from surface oxides. Some of this is due to volatile oxides; but Krikorian [5] points out that the presence of moisture in laboratory air could also create high volatility hydroxides and oxy-hydroxides during high temperature exposure.

A number of authors have studied chromia vaporization experimentally and provided supporting thermodynamic calculations. It is well-known that chromia vaporizes in an oxidative environment [6-8]:

Cr$_2$O$_3$(s) + 3/2 O$_2$(g) = 2 CrO$_3$(g)   (4)
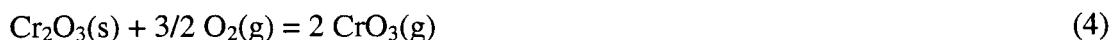
A plot of the vapor pressure of CrO$_3$(g) from Cr$_2$O$_3$ with 21% O$_2$/79% Ar is shown in Figure 1. The addition of 10% water vapor enhances volatility even further from the reaction [8,9]:

Cr$_2$O$_3$(s) + 2 H$_2$O(g) + 3/2 O$_2$(g) = 2 CrO$_2$(OH)$_2$(g)   (5)
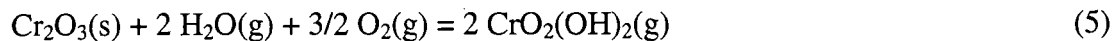
The vapor pressure of $CrO_2(OH)_2(g)$ from $Cr_2O_3(s)$ + 21% O_2/10% H_2O/69% Ar is also shown in Figure 1. Note the higher vapor pressure of $CrO_2(OH)_2(g)$ than $CrO_3(g)$. Similar oxy-hydroxides from Mo and W are thought to play a role in the degradation of Mo emitter materials [10] and W filaments in lamps [2].

Boron is commonly proposed as a constituent in high temperature materials. Transition metal borides have extremely high melting points [11], boron is used as an oxidation inhibiter in carbon [12], and boron nitride (BN) is used as a fiber coating in continuous fiber reinforced ceramic matrix composites [13]. However, the oxy-hydroxide of boron forms readily from boric oxide:

$$B_2O_3(s) + H_2O(g) = 2\ BO(OH)(g) \tag{6}$$

The BN fiber coating in composites has been observed to vaporize [13] in moisture-containing environments at temperatures as low as 500°C , very likely by BN oxidation to B_2O_3 and subsequent vaporization to $BO(OH)(g)$.

Silicon-based ceramics, such as silicon carbide (SiC) and silicon nitride (Si_3N_4), and composites of these are promising high temperature materials. These materials rely on a thin film of thermally grown silica (SiO_2) for corrosion protection. In dry oxygen, this film is remarkably durable, however in high-temperature water-vapor containing environments, this film vaporizes according to:

$$SiO_2(s) + H_2O(g) = Si(OH)_4(g) \tag{7}$$

Oxidation of the SiC or Si_3N_4 substrate occurs concurrently with the volatilization reaction (7) and can lead to substantial material loss over long periods of time [14-16].

There is also evidence of volatile hydroxide formation with Al_2O_3 and ZrO_2. Tai et al. [17] have observed substantially more grain boundary etching on Al_2O_3 in an Ar/H_2O environment as compared to a pure Ar environment at 1700°C. This is attributed to

$Al(OH)_3(g)$ formation. Etori et al. [18] have observed weight losses of Al_2O_3 and ZrO_2 in a petroleum gas burner at 1500°C, 1.8 bar total pressure, and a gas velocity of 150 m/s. The gas atmosphere contained 9.5% H_2O. They suggested the possibility of metal hydroxide formation, although no further evidence such as a downstream deposit was observed. Recently, Yuri and Hisamatu [19] have done further studies on Al_2O_3 weight loss in a burner and observed a water vapor pressure dependence of near 1.5, suggesting the reaction:

$$\tfrac{1}{2}\, Al_2O_3 + 3/2\, H_2O(g) = Al(OH)_3(g) \tag{8}$$

In summary there are a number of applications where volatile hydroxides play a key role. Thus it is essential to understand the thermodynamics of these species so we can predict their corrosion rates.

Techniques for Studying Thermodynamics of Metal Hydroxides

Thermodynamic studies of metal hydroxides require highly oxidizing environments and the most common method for studies of high temperature vapors, based on the Knudsen cell, requires a more reducing environment. Hence the Knudsen cell technique must be adapted for water vapor studies. There are several studies in the literature of hydroxides using gas-leak Knudsen cell mass spectrometry [20-27] . Here a small amount of water vapor is admitted to a Knudsen cell to react with an oxide. Alternatively $H_2(g)$ or $D_2(g)$ may be admitted which reacts with the oxide to form $H_2O(g)$ or $D_2O(g)$ and the metal hydroxides. The volatile products are then characterized with the mass spectrometer. There are pressure limitations on this techniques as the ionizer and detector of the instrument cannot tolerate $P(H_2O)$ greater than $\sim 10^{-5}$ bar.

A free jet-sampling mass spectrometer (FJSMS) can directly sample a 1 bar chemical process in an oxidizing environment. This type of instrument has been described in detail elsewhere [28-29] and the principle will be briefly summarized here. The system consists of a series of differentially pumped vacuum chambers. In our system, the reaction occurs

in a tube furnace adjacent to a small orifice in a Pt-Rh sampling cone. The gas species enter the orifice and undergo a free jet expansion. An abrupt transition to molecular flow occurs and the molecular beam is directed to a mass spectrometer. The actual expansion process is quite complex and dependent on the mass of the vapor species. We use a quadrupole mass spectrometer, which further introduces mass discrimination effects. Hence conversion of ion intensities to absolute pressures cannot be easily done. We use our instrument only for qualitative determinations of the amounts of volatile hydroxides and oxy-hydroxides [30].

The most valuable quantitative technique for obtaining thermodynamic data on hydroxides is the transpiration method [31]. A carrier gas entrains an equilibrium vapor and transports it to a low temperature portion of the system where it condenses. This amount of condensate is accurately determined by an appropriate analytical technique. From the amount of condensate and assuming the vapor specie is known, the vapor pressure of that species can be calculated. This vapor pressure can be calculated as a function of water vapor pressure to confirm the species' identity and as a function of temperature to obtain thermodynamic data. Flow rates are set to avoid surface reaction kinetic limitations and gas phase diffusion limitations on the reaction rate. Among the first studies of hydroxides with this technique are those of Glemser and colleagues [32-34]. Belton and colleagues [35-37] have also used transpiration to study transition metal hydroxides. More recently Hashimoto [38] has used the transpiration method to study Ca, Si, and Al hydroxides. He uses a Pt/Rh transpiration cell.

Our transpiration apparatus [39] is shown schematically in Figure 2. We also use a Pt/Rh transpiration cell. We use a peristaltic pump to inject water into the gas stream. An argon blanket gas flows in the region between the furnace tube and the transpiration cell. The blanket gas is monitored with a residual gas analyzer to detect any leaks in the system.

Metal hydroxides have also been studied in hydrogen-oxygen flames using spectroscopic techniques. The metals often form mono-hydroxides such as CuOH, GaOH, and InOH

[40-41]. These studies yield data over a wide range of temperature, but proper identification of spectral lines may be difficult.

Thermal functions for many metal hydroxides have been estimated treating the hydroxyl group as a pseudo halide [2, 23, 42-46]. Various correlations have been established between fluoride or chloride and corresponding hydroxide bond strengths. Vibrational frequencies and molecular shapes for hydroxides have also been taken from fluorides and chlorides.

Ab initio methods of quantum chemistry should yield more accurate thermal functions for hydroxides [47, 48]. Baushlicher et al. [47] have calculated dissociation energies and shapes of the alkali and alkaline-earth mono-hydroxides. They conclude that the more ionic hydroxides are linear and the more covalent hydroxides are bent. This is consistent with experimental data [49, 50]. Allendorf et al. [48] use *ab initio* methods to calculate thermal functions for a variety of Si-O-H species. Their results will be compared to our experimental data in a later section.

Review of Thermodynamics of Metal Hydroxides

There are only a few reviews in the literature on the thermodynamics of volatile metal hydroxides [1,2, 42, 51, 52]. The authors of these reviews look for periodic trends in thermodynamic stabilities; however given the limited experimental data it is difficult to find these trends. Some element groups in the periodic table do lead to highly stable volatile hydroxides and/or oxy-hydroxides.

Table I presents available experimental enthalpies ($\Delta_r H^o(298)$) and entropies ($\Delta_r S^o(298)$) for a series of hydroxide formation reactions from the condensed phase oxide, i.e. reaction (2). The condensed phase oxide with the highest metal oxidation state was selected, e.g. Fe_2O_3 for Fe. Only data for experimentally observed gaseous hydroxide or oxy-hydroxide species are listed in the table. When the data appeared to be estimated,

they are not listed. Note that for the Group I hydroxides, with the exception of Li(OH)(g) and Li(OH)$_2$(g) [21], form by direct vaporization only (reaction (1)) and this reaction is given.

For all the reactions, a more favorable change in free energy is attained by a lower $\Delta_r H°(298)$ and a higher $\Delta_r S°(298)$. For this approximation, we assume a constant $\Delta_r H°$ and $\Delta_r S°$ with temperature. Note also that at higher temperatures the $T\Delta_r S°$ term in free energy becomes more important and the particular reaction will be more important [2].

Table I also gives an estimate of metal-hydroxide group bond energies at 298.15 K from these experimental data. These bond energies were estimated [5] from:

$$MOH(g) = M(g) + OH(g) \qquad (9a)$$
$$M(OH)_2(g) = M(g) + 2\,OH(g) \qquad (9b)$$
$$MO(OH)_2(g) = MO(g) + 2\,OH(g) \qquad (9c)$$
$$MO_2(OH)_2(g) = MO_2(g) + 2\,OH(g) \qquad (9d)$$
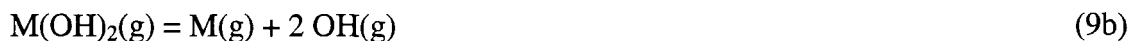
The bond energies are useful to compare the strengths of the metal-hydroxide group bond for the various species.

For the data taken from the JANAF [45] and IVTAN [46] tables, the $\Delta_r H(298)$, $\Delta_r S(298)$ and bond energy could be readily calculated. For the data taken from other sources, these quantities were calculated from the vapor pressures and partition functions. Vibrational frequencies, interatomic distances, and bond angles were taken from the sources cited.

In surveying the literature, we found some controversy in the shape of the metal-oxygen-hydrogen bond. Consider first the simple mono-hydroxides. As noted, *ab initio* calculations [47] indicate that metal mono-hydroxides with ionic metal/hydroxide bonds are linear; whereas the metal/hydroxide bond is bent if it has a larger degree of covalent character. This *ab initio* study [47] shows that all alkali and alkaline-earth mono-hydroxides are linear, except for BeOH, which has a larger degree of covalency.

Recent spectroscopic studies on CuOH and AgOH indicate a bent structure [50]. It is likely that all the transition elements form hydroxides with bent M-O-H structures. Ebbinghaus [44] assumes a bent structure for Cr-O-H in all the various chromium hydroxides and oxy-hydroxides for which he estimates thermal functions. In our literature search, we found some calculations done for linear structures of transition metal hydroxides and some for bent structures. For these situations where there is some controversy about the shape of the molecule, we have done the 'third law' calculation for both a linear and bent molecule, using the spectroscopic data discussed above. The two different molecular shapes result in two different calculated moments of inertia, which in turn lead to different rotational partition functions. Compare the linear and bent molecules in Table I. Note that heat of reaction is generally increased about 20 kJ/mol, the entropy of reaction is increased about 20 J/mol-K and the calculated bond energy is decreased about 20 kJ/mol in changing from a linear to a bent molecule.

The possibility of a bent M-O-H bond on the di-hydroxides is less well-studied. There does not seem to be experimental data on the shapes of any of these species. In general if the M-O-H bond is bent in the mono-hydroxide; it is assumed to be bent in the di-hydroxide. The presence of an additional hydroxide group suggests an internal rotation—either free or hindered. Ebbinghaus [44] assumes the $Cr(OH)_2(g)$ has free internal rotations and the higher hydroxides have hindered rotations. So now the altered moments of inertia and internal rotations have a larger impact on the partition function. Note the large effect on the enthalpy, entropy, and bond energy for $Mn(OH)_2(g)$, shown in Table I.

This brief review has several findings:
1. The only complete data sets are for groups IA, IIA, VIA, and IIIB.
2. With the exception of the first row, the bond energies for groups IA and IIA are fairly constant.
3. For group IIIB, the hydroxides become less stable with increasing atomic number.

4. Group VIA tends to form highly stable oxy-hydroxides. Here with increasing atomic number they become less stable.

5. There are also several exceptionally stable hydroxides and oxy-hydroxides. These are $Be(OH)_2$, $BO(OH)$, $B(OH)_2$ and the Group VIA oxy-hydroxides.

6. Theoretical evidence and spectroscopic evidence indicate that the mono-hydroxides with ionic bonding are linear; whereas the mono-hydroxides with more covalent bonding are bent. Recalculation of the partition functions for the transition metal hydroxides assuming a bent metal/hydroxide bond will yield a more accurate thermal functions.

Experimental Study of the Si-O-H System

In the last part of this paper, we discuss our recent experimental work on the Si-O-H system. We use both transpiration and free jet expansion mass spectrometry, as discussed in the experimental section. Transpiration studies were done over a range of temperatures and pressures. Thermodynamic quantities were derived from both the second and third law methods.

There are a number of possible reactions in this system [43]:

$$SiO_2(s) + \tfrac{1}{2} H_2O(g) = SiO(OH)(g) + \tfrac{1}{4} O_2(g) \tag{10a}$$

$$SiO_2(s) + H_2O(g) = SiO(OH)_2(g) \tag{10b}$$

$$SiO_2(s) + 2 H_2O(g) = Si(OH)_4(g) \tag{10c}$$

$$2 SiO_2(s) + 3 H_2O(g) = Si_2O(OH)_6(g) \tag{10d}$$
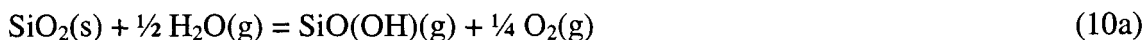
There are two sets of calculated data for these species. One is based on treatment of the hydroxyl group as a pseudo-halide [43]; the other is based on *ab initio* methods [48]. These results are plotted as function of temperature in Figure 3. The vapor pressures of $Si(OH)_4$ show reasonable agreement; however there is clear disagreement on the vapor pressures of $SiO(OH)$ and $SiO(OH)_2$.

As noted, Hashimoto [38] has done a precise transpiration study of the Si-O-H system from 1173-1773 K. His pressure dependent experiments indicate that $Si(OH)_4$ is the

dominant vapor species. He derives second law enthalpies and entropies from his measurements. We did a transpiration and mass spectrometry study to look further at the identity of the vapor species and also obtain third law enthalpies, based on the *ab initio* thermal functions of Allendorf et al. [48].

Our transpiration apparatus has been described earlier in this paper. The deposits of Si containing species on the Pt/Rh collection tube were dissolved in a solution of 4% HF at 50°C. The solution was then analyzed with plasma emission spectroscopy. The lower limit of detection was about 20 μg of Si. The amount of Si containing condensate was converted to vapor pressure by considering the flow rate of the argon carrier gas, water vapor, and the Si vapor species. Consider first the molar flow rate of Ar, Q_{Ar}, entering the furnace (position 1) before water is introduced:

$$Q_{Ar} = \frac{P_1 f_1}{RT_1} \qquad (11)$$

Here P is the pressure, f is the volume flow rate, R is the gas constant, and T is the absolute temperature. The volume flow rate entering the reaction chamber (position 2) is given by

$$f_2 = \frac{T_2}{P_2} R [Q_w + Q_{Ar}] \qquad (12)$$

Here Q_w is the molar flow rate of water. The volume flow rate leaving the reaction chamber (position 3) is simply expression (12) with the addition of Q_{Si}. This is small in comparison to $Q_w + Q_{Ar}$, so we can take $f_3 = f_2$. Finally the pressure of Si species leaving the reaction chamber (position 3) is given by:

$$\frac{P_{Si}}{P_T} = \frac{Q_{Si}}{Q_{Ar} + Q_w + Q_{Si}} \qquad or \qquad \frac{P_{Si}}{P_T} = \frac{Q_{Si} RT_3}{f_3} \qquad (13)$$

Q_{Si} is calculated from the amount of Si in the deposit collected.

In these transpiration experiments the identity of the vapor species are best determined by the dependence of pressure of Si-O-H species on the partial pressure of water vapor. For the formation of $Si(OH)_4$ according to reaction (10c) a plot of log P(Si-OH) vs log P(H_2O) should yield a slope of 2. For the formation of $SiO(OH)_2$ according to reaction (10b) such a plot should yield a slope of 1. The results are shown in Figure 4 for 1073,

1273, and 1473 K. The lower temperatures have a slope close to 2; but the high temperature has a slope of 1.69. Thus at lower temperatures, $Si(OH)_4$ appears to be the dominant specie; whereas at higher temperatures a second specie, very likely $SiO(OH)_2$, is also important. It can be shown that an exponent of 1.69 corresponds to 0.31 $SiO(OH)_2(g)$ and 0.69 $Si(OH)_4(g)$ [39].

These results are consistent with studies in our free-jet expansion mass spectrometer. Hydroxides also behave like pseudo-halogens in mass spectrometer fragmentation processes. Thus a typically observed ion is formed by the removal of one hydroxyl group from the parent. The major ions were $Si(OH)_3^+$ and $SiO(OH)^+$, which correspond to $Si(OH)_4$ and $SiO(OH)_2$, respectively.

Having identified $Si(OH)_4$ as the major specie to about 1373 K, we can then obtain a second law heat and entropy from the van't Hoff equation:

$$ ln\,K = \frac{-\Delta H^o}{R}\left(\frac{1}{T}\right) + \frac{\Delta S^o}{R} \qquad with \qquad K = \frac{P(\,Si(\,OH\,)_4\,)}{[\,P(\,H_2O\,)]^2} \qquad [14] $$

The results are shown in Figure 5 and Table II. Values from the calculations of Allendorf et al. [48] and experimental measurements of Hashimoto [38] are shown for comparison and the agreement is very good.

The calculations of Allendorf et al. allow the derivation of the free energy function for a third law calculation of $\Delta_r H^o(298)$. Allendorf's calculation leads to the $Si(OH)_4$ structure with symmetry group C_1 and four hindered internal rotations. His numbers for the enthalpy of formation at 298.15 K and free energy of formation were fitted to a polynomial of IVTAN form [46]. This was combined with the IVTAN data for Si, O_2, H_2 to yield the free energy function of $Si(OH)_4$:

$$ FEF(\,Si(\,OH\,)_4\,) = \; -2234.21313 + -662.11547 * ln(T/10000) + 0.124 * (T/10000)^{-2} + $$
$$ -22.89238 * (T/10000)^{-1} + 7126.04925 * (T/10000) + -24458.89172 * (T/10000)^2 $$
$$ + 40760.17257 * (T/10000)^3 \qquad\qquad [15] $$

This was used with the standard third law equation to calculation an enthalpy of reaction for reaction (10c):

$$\Delta_r H^o(298) = \Delta G^o(T) - T\,\Delta\left(\frac{G^o(T) - H^o(298)}{T}\right) = RT\ln K_p - T\,\Delta\left(FEF^o(298)\right) \quad [16]$$

Twenty nine data points from our transpiration study were used to calculate an enthalpy and the results are shown in Table II. The agreement with Allendorf's calculations is excellent.

Summary and Conclusions

Volatile metal hydroxides are important in a number of high temperature corrosion processes. Examples of these have been discussed. Thermodynamic data on these species are limited, in part due to the complexities of thermodynamic measurements in oxidizing environments. Gas leak Knudsen cell mass spectrometry, free-jet sampling mass spectrometry, transpiration, and H_2/O_2 flames are the commonly used experimental techniques. Theoretical predictions of thermodynamic quantities for these metal hydroxides and oxy-hydroxides have been made using the pseudo halogen behavior of the hydroxyl group. More recently, *ab initio* methods have been applied to obtain thermodynamic quantities. An important result from the latter is that the ionic mono-hydroxides tend to have linear M-O-H bonding and the more covalent hydroxides tend to have bent M-O-H bonding.

Available experimental data on metal hydroxides have been discussed. From these data, enthalpies and entropies of formation from water vapor and the most stable oxide are calculated as well as metal/hydroxide bond energies. Although experimental data on many hydroxides are unavailable, some trends can be observed. With the exception of the first row, groups IA and IIA have fairly constant metal hydroxide bond energies. For group IIIB, the metal hydroxide bond energy decreases with increasing atomic number. There are also several exceptionally stable hydroxides and oxy-hydroxides. These are $Be(OH)_2$, $BO(OH)$, $B(OH)_2$ and the Group VIA oxy-hydroxides.

Studies from our laboratories on the Si-O-H system are discussed. Transpiration and free-jet sampling mass spectrometry are used. It appears that $Si(OH)_4$ is the dominant

vapor specie to about 1373 K; above that $SiO(OH)_2$ may be important. A second law enthalpy and entropy and a third law enthalpy for the reaction of water vapor and SiO_2 to form $Si(OH)_4$ are reported. These compare favorably with theoretical calculations [48] and previous experimental data [38].

Acknowledgements

Group	Reaction	$\Delta_r H^o_{298}$ kJ/mol	$\Delta_r S^o_{298}$ J/mol-K	$D^o_{298}(M-OH)$ kJ/mol	Geometry of M-OH Bond	Reference
IA	$Li_2O(s) + H_2O(g) = 2\ Li(OH)(g)$	186	97	433	Linear	JANAF [45]
	$NaOH(s) = NaOH(g)$	228	163	344	Linear	JANAF [45]
	$KOH(s) = KOH(g)$	192	157	360	Linear	JANAF [45]
	$RbOH(s) = RbOH(g)$	177	156	361	Linear	IVTAN [46]
	$CsOH(s) = CsOH(g)$	157	156	374	Linear	JANAF [45]
IIA	$BeO(s) + \frac{1}{2}\ H_2O(g) = Be(OH)(g) + \frac{1}{4}\ O_2(g)$	614	153	477	See text	JANAF [45]
	$BeO(s) + H_2O(g) = Be(OH)_2(g)$	174	31	539	See text	JANAF [45]
	$MgO(s) + \frac{1}{2}\ H_2O(g) = Mg(OH)(g) + \frac{1}{4}\ O_2(g)$	557	156	350	Linear	JANAF [45]
	$MgO(s) + H_2O(g) = Mg(OH)_2(g)$	271	52	399	Linear	JANAF [45]
	$CaO(s) + \frac{1}{2}\ H_2O(g) = Ca(OH)(g) + \frac{1}{4}\ O_2(g)$	562	154	410	Linear	JANAF [45]
	$CaO(s) + H_2O(g) = Ca(OH)_2(g)$	266	59	433	Linear	JANAF [45]
	$SrO(s) + \frac{1}{2}\ H_2O(g) = Sr(OH)(g) + \frac{1}{4}\ O_2(g)$	507	148	408	Linear	JANAF [45]
	$SrO(s) + H_2O(g) = Sr(OH)_2(g)$	238	61	434	Linear	JANAF [45]
	$BaO(s) + \frac{1}{2}\ H_2O(g) = Ba(OH)(g) + \frac{1}{4}\ O_2(g)$	443	138	444	Linear	JANAF [45]
	$BaO(s) + H_2O(g) = Ba(OH)_2(g)$	163	54	442	Linear	JANAF [45]
VIA	$\frac{1}{2}\ Cr_2O_3(s) + \frac{1}{2}\ H_2O(g) = CrOH(g) + \frac{1}{2}\ O_2(g)$	747 770	213 227	380 358	Linear Bent	Gorokhov et al. [23]
	$\frac{1}{2}\ Cr_2O_3(s) + H_2O(g) + 3/4\ O_2(g) = CrO_2(OH)_2(g)$	61	-26	375	Bent	Ebbinghaus [44]
	$MoO_3(s) + H_2O(g) = MoO_2(OH)_2(g)$	135	89	460		JANAF [45]
	$WO_3(s) + H_2O(g) = WO_2(OH)_2(g)$	530	87	530		JANAF [45]

VIIA	$MnO_2(s) + \frac{1}{2} H_2O(g) = Mn(OH)(g) + \frac{3}{4} O_2(g)$	641.54 663.96	253.71 268.33	322.42 300.01	Linear Bent	Hildenbrand and Lau [24]
	$MnO_2(s) + \frac{1}{2} H_2O(g) = MnO(OH)(g) + \frac{1}{4} O_2(g)$	469.87 469.18	205.79 218.74	372.21 372.89	Linear Bent	Hildenbrand and Lau [24]
	$MnO_2(s) + H_2O(g) = Mn(OH)_2(g) + \frac{1}{2} O_2(g)$	362.82 442.08	289.04 310.63	361.03 322.38	Linear Bent	Hildenbrand and Lau [24]
VIII	$\frac{1}{2} Fe_2O_3(s) + \frac{1}{2} H_2O(g) = Fe(OH)(g) + \frac{1}{2} O_2(g)$	652.80 668.79	213.37 228.59	334.31 318.32	Linear Bent	Murad [22]
	$\frac{1}{2} Fe_2O_3(s) + H_2O(g) = Fe(OH)_2(g) + \frac{1}{4} O_2(g)$	324.04	153.13	439.22	Bent	Belton and Richardson [35] JANAF [45]
IB	$CuO(s) + \frac{1}{2} H_2O(g) = Cu(OH)(g) + \frac{1}{4} O_2(g)$	400.02 429.47	145.49 160.99	259.84 230.39	Linear Bent	Belyaev et al. [40]
IIB	$ZnO(s) + H_2O(g) = Zn(OH)_2(g)$	201.39	54.89	300	Bent	Glemser et al. [32]
IIIB	$\frac{1}{2} B_2O_3(s) + \frac{1}{2} H_2O(g) = BO(OH)(g)$	196	118	600		JANAF [45]
	$\frac{1}{2} B_2O_3(s) + H_2O(g) = B(OH)_2(g) + \frac{1}{4} O_2(g)$	401	84	557		JANAF [45]
	$\frac{1}{2} B_2O_3(s) + 3/2 H_2O(g) = B(OH)_3(g)$	6.4	-15	556		JANAF [45]
	$\frac{1}{2} Al_2O_3(s) + \frac{1}{2} H_2O(g) = Al(OH)(g) + \frac{1}{2} O_2(g)$	779	199	549		IVTAN [45]
	$\frac{1}{2} Al_2O_3(s) + \frac{1}{2} H_2O(g) = AlO(OH)(g)$	498	134	566		JANAF [45]
	$\frac{1}{2} Al_2O_3(s) + H_2O(g) = Al(OH)_2(g) + \frac{1}{4} O_2(g)$	572	121	458		IVTAN [46]
	$\frac{1}{2} Al_2O_3(s) + 3/2 H_2O(g) = Al(OH)_3(g)$	188	-7.3	487		Hashimoto/ IVTAN [38, 46]

	½ Ga_2O_3(s) + ½ H_2O(g) = Ga(OH)(g) + ½ O_2(g)	549.62 569.74	210.65 223.58	428.15 408.02	Linear Bent	Kelly and Padley [41]
	½ In_2O_3(s) + ½ H_2O(g) = In(OH)(g) + ½ O_2(g)	493.92 513.11	215.43 228.04	368.54 349.36	Linear Bent	Kelly and Padley [41]
IVB	SiO_2(s) + ½ H_2O(g) = SiO(OH)(g) + ¼ O_2(g)	675.12 718.12	190.04 187.62	297 254	Linear Bent	Hildenbrand and Lau [25,26]
	SiO_2(s) + H_2O(g) = SiO(OH)$_2$(g)	260.42 316.78	61.62 64.46	435.9 408	Linear Bent	Hildenbrand and Lau [25, 26]
	SiO_2(s) + 2 H_2O(g) = Si(OH)$_4$(g)	55.30	-76.18	486.61	Bent	This study

Table I. Thermodynamic data on metal hydroxides.

Study	T(K)	$\Delta_r H$ (kJ/mol)	$\Delta_r S$ (J/mol-K)
Hashimoto—Second Law	1600	56.7 ± 1.7	-66.2 ± 1.0
Allendorf—Second Law	1200	57.02	-64.8
This Study	1200	54.5 ± 2.8	-67.6 ± 2.2
Allendorf	298.15	55.3	
Krikorian	298.15	56.5	
This Study—Third Law	298.15	58.4 ± 3.6	

Table II. Enthalpies and entropies for the reaction SiO_2(cristobalite) + 2 H_2O(g) = $Si(OH)_4$(g).

References:

1. O. Glemser and H. G. Wendlandt, in H. J. Emeléus and A. G. Sharpe (Eds.), Advan. Inorg. Chem. Radiochem. Vol. 5, 1963, pp. 215-54.

2. J. W. Hastie, High Temperature Vapors Science and Technology, Ch 2 and 5, Academic Press, New York, 1975.

3. N. S. Jacobson, Corrosion of Silicon-Based Ceramics in Combustion Environments, J. Am. Ceram. Soc. 76 (1993), 3-28.

4. I. Zaplatynsky, Volatilization of Oxides During Oxidation of Some Superalloys at 1200° C, Oxid. Met. 11 (1977), 289-305.

5. O. H. Krikorian, Predictive calculations of volatilities of metals and oxides in steam-containing environments, H. Temp-H. Press 14 (1982), 387-97.

6. H. C. Graham and H. H. Davis, Oxidation/Vaporization Kinetics of Cr_2O_3, J. Am. Ceram. Soc. 54 (1971), 89-93.

7. C. E. Lowell and W. A. Sanders, Mach 1 Oxidation of Thoriated Nickel Chromium at 1204° C (2200° F), NASA Technical Note (1971), TN D-6562.

8. F. J. Kohl and C. A. Stearns, Vaporization of Chromium Oxides from Surface of TD-NiCr Under Oxidizing Conditions, NASA Technical Memorandum (1970) TM X-52879.

9. G. C. Fryburg, R. A. Miller, F. J. Kohl, and C. A. Stearns, Volatile Products in the Corrosion of Cr, Mo, Ti, and Four Superalloys Exposed to O_2 Containing H_2O and Gaseous NaCl, J. Electrochem. Soc. 124 (1977), 1738-43.

10. G. Wahl and P. Batzies, Evaporation of Molybdenum in Vacuum, in O_2-, and in H_2O-Atmospheres, in IEEE Conference Record of 1970 Thermionic Conversion Specialist Conference, Miami Beach, FL, IEEE, New York, pp. 119-21.

11. R. L. Fleischer, High-Temperature, High-Strength Materials—An Overview, J. Met. (Dec 1985), 16-20.

12. J. Buchanan and J. A. Little, Glass sealants for carbon-carbon composites, J. Mat. Sci. 28 (1993), 2324-2330.

13. N. S. Jacobson, G. N. Morscher, D. R. Bryant, and R. E. Tressler, High-Temperature Oxidation of Boron Nitride: II, Boron Nitride Layers in Composites, J. Am. Ceram. Soc. 82 (1999), 1473-82.

14. E. J. Opila and R. E. Hann, Paralinear Oxidation of CVD SiC in Water Vapor, J. Am. Ceram. Soc. 80 (1997), 197-205.

15. R. C. Robinson and J. L. Smialek, SiC Recession Caused by SiO_2 Scale Volatility under Combustion Conditions: Part I, Experimental Results and Empirical Model, J. Am. Ceram. Soc. 82 (1999), 1817-25.

16. E. J. Opila, J. L. Smialek, R. C. Robinson, D. S. Fox, and N. S. Jacobson, SiC Recession Caused by SiO_2 Scale Volatility under Combustion Conditions: Part II, Thermodynamics and Gaseous-Diffusion Model, J. Am. Ceram. Soc. 82 (1999), 1826-34.

17. W.-P. Tai, T. Watanabe, and N. S. Jacobson, High-Temperature Stability of Alumina in Argon and Argon/Water-Vapor Environments, J. Am. Ceram. Soc. 82 (1999), 245-48.

18. Y. Etori, T. Hisamatsu, I. Yuri, Y. Yasutomi, T. Machida, and K. Wada, Oxidation Behavior of Ceramics for Gas Turbines in Combustion Gas Flow at 1500°C, International Gas Turbine and Aeroengine Congress and Exhibition, Orlando, FL, June 2-5, 1997, Paper 97-GT-355.

19. I. Yuri and T. Hisamatsu, Recession Rate Prediction for Ceramic Materials in Combustion Gas Flow, Proceedings of ASME TURBO EXPO 2003, June 16-19, Atlanta, GA, Paper GT2003-38886.

20. D. J. Meschi, W. A. Chupka, and J. Berkowitz, Heterogeneous Reactions Studied by Mass Spectrometry. I. Reactions of $B_2O_3(s)$ with $H_2O(g)$, J. Chem. Phys. 33 (1960), 530-33.

21. J. A. Berkowitz, D. J. Meschi, and W. A. Chupka, Heterogeneous Reactions Studied by Mass Spectrometry. II. Reaction of $Li_2O(s)$ with $H_2O(g)$, J. Chem. Phys. 33 (1960), 533-40.

22. E. Murad, "Thermochemical properties of gaseous FeO and FeOH," J. Chem. Phys. 73 (1980), 1381-85.

23. L. N. Gorokhov, J. I. Milushin, and A. M. Emelyanov, Knudsen Effusion Mass Spectmetric Determination of Metal Hydroxide Stabilities, H. Temp. Sci. 26 (1990), 395-403.

24. D. L. Hildenbrand and K. H. Lau, Thermochemistry of gaseous manganese oxides and hydroxides, J. Chem. Phys. 1000 (1994), 8377-80.

25. D. L. Hildenbrand and K. H. Lau, Thermochemistry of gaseous SiO(OH), $SiO(OH)_2$, and SiO_2, J. Chem. Phys. 101 (1994), 6076-79.

26. D. L. Hildenbrand and K. H. Lau, Comment on "Thermochemistry of gaseous SiO(OH), SiO(OH)$_2$, and SiO$_2$," [J. Chem. Phys. 101, 6076 1994], J. Chem. Phys. 108 (1998), 6535.

27. M. Farber, R. D. Srivastava, M. A. Frisch and S. P. Harris, Mass Spectrometer Studies of Al + H$_2$O Reactions in Effusion Cells and in Atmospheric H$_2$ + O$_2$ Flames, in High Temperature Studies in Chemistry, Faraday Symposia of the Chemical Society No. 8, 1973, pp. 121-130.

28. C. A. Stearns, F. J. Kohl, G. C. Fryburg, and R. A. Miller in J. W. Hastie [Ed.] Characterization of High Temperature Vapors and Gases, NBS Special Publication No. 561, National Bureau of Standards, Washington, D. C., 1978, pp. 303-55.

29. Applications of Free-Jet, Molecular Beam, Mass Spectrometric Sampling Proceedings, Estes Park, CO, October 11-14, 1994, NREL-CP_433-7748.

30. E. J. Opila, D. S. Fox, and N. S. Jacobson, "Mass Spectrometric Identification of Si-O-H(g) Species from the Reaction of Silica with Water Vapor at Atmospheric Pressure," J. Am. Ceram. Soc. 80 (1997), 1009-12.

31. U. Merten and W. E. Bell, in J. L. Margrave [Ed.], The Characterization of High Temperature Vapors, J. Wiley and Sons, Inc., New York, 1967. pp. 91-114.

32. O. Glemser, H. G. Völz, and B. Meyer, Gasförmge Hydroxyde. II. Über gasförmiges Zinkhydroxyd, Z. anorg. allgem. chem. 192 (1957), 311-24.

33. O. Glemser and R. V. Haeseler, Über gasförmiges Hydroxide des Molybdäns und Wolframs, Z. anorg. allgem. chem. 316 (1962), 169-81.

34. O. Glemser and A. Müller, Über ein gasförmiges Hydroxid des Chroms, Z. anorg. allgem. chem. 334, (1964) 150-54.

35. G. R. Belton and F. D. Richardson, A Volatile Iron Hydroxide, Trans. Far. Soc. 58 (1962), 1562-72.

36. G. R. Belton and R. L. McCarron, The Volatilization of Tungsten in the Presence of Water Vapor, J. Phys. Chem. 68 (1964), 1852-56.

37. Y-W. Kim and G. R. Belton, "The Thermodynamics of Volatilization of Chromic Oxide: Part I. The Species CrO$_3$ and CrO$_2$OH," Met. Trans. 5 (1974), 1811-16.

38. A. Hashimoto, "The effect of H_2O gas on volatilities of planet-forming major elements: I. Experimental determination of thermodynamic properties of Ca-, Al-, and Si-hydroxide gas molecules and its application to the solar nebula," Geochim. Cosmochim. Acta, 56 (1992), 511-32.

39. E. Copland, D. Myers, E. J. Opila, and N. S. Jacobson, in M. McNallan and E. Opila [Eds.] High Temperature Corrosion and Materials Chemistry III, Proceedings of the International Symposium, The Electrochemical Society, Pennington, NJ, 2001, pp. 253-61.

40. V. N. Belyaev, N. L. Lebedeva, K. S. Krasnov, and L. V. Gurvich, Computation of copper oxide and hydroxide dissociation energy by the flame spectrophotometry method, Izvestiya vuzov. Khimiya i khim. tekhnol. 21 (1978), 1698-1700.

41. R. Kelly and P. J. Padley, Photometric Studies in Hydrogen + Oxygen + Carbon Dioxide Flames, Trans. Faraday Soc. 67 (1971), 740-49.

42. D. D. Jackson, Thermodynamics of the Gaseous Hydroxides, UCRL-51137, Lawrence Livermore Laboratory, 1970.

43. O. H. Krikorian, Thermodynamics of the Silica-Steam System, Presented at Symposium on Engineering with Nuclear Explosives, CONF-700101, May 1970.

44. B. B. Ebbinghaus, Thermodynamics of Gas Phase Chromium Species: The Chromium Oxides, the Chromium Oxyhydroxides, and Volatility Calculations in Waste Incineration Processes, Comb. and Flame 93 (1993), 119-37.

45. M. W. Chase, NIST-JANAF Thermochemical Tables, Journal of Physical and Chemical Reference Data, Monograph No. 9, American Institute of Physics, Woodbury, New York, 1999.

46. L. V. Gurvich, V. S. Iorish, D. V. Chekhovskoi, and V. S. Yungman, IVTANTHERMO—A Thermodynamic Database and Software System for the Personal Computer, NIST Special Database 5, U. S. Department of Commerce, Gaithersburg, MD, 1993.

47. C. W. Bauschlicher, Jr., S. R. Langhoff, and H. Partridge, "*Ab initio* study of the alkali and alkaline-earth monohydroxides," J. Chem. Phys. 84, 901-9 (1986).

48. M. D. Allendorf, C. F. Melius, P. Ho, and M. R. Zachariah, Theoretical Study of the Thermochemistry of Molecules in the Si-O-H System, J. Phys. Chem. 99 (1999), 15284-93.

49. R. L. Kuckowski, D. R. Lide, Jr., and L. C. Krisher, Microwave Spectra of Alkali Hydroxides: Evidence for Linearity of CsOH and KOH, J. Chem. Phys. 44 (1966), 3131-32.

50. C. J. Whitham, J. Ozeki, and S. Saito, "Microwave spectroscopic detection of transition metal hydroxides: CuOH and AgOH," J. Chem. Phys. 110 (1999), 11109-112.

51. G. Elliot, Gaseous Hydrated Oxides, Hydroxides, and other Hydrated Molecules, UCRL-1831, PhD Thesis, University of California at Berkeley, 1952.

52. T. Greene, S. P. Randall, and J. L. Margrave, Characterization of Unusual Gaseous Oxide and Hydroxide Molecules in M-O-H Systems at High Temperatures, in Thermodynamic and Transport Properties of Gases, Am. Soc. Mech. Eng., 1959, pp. 222-25.

Vapor Species over Chromia
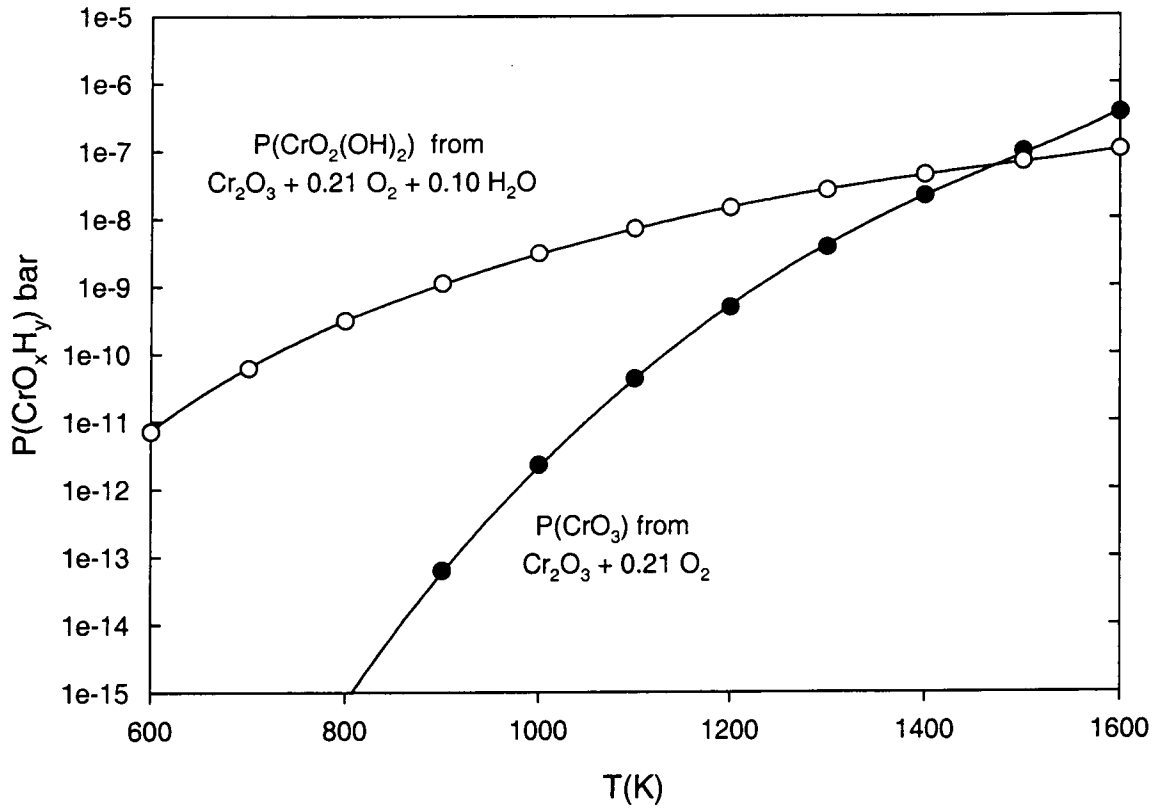
Figure 1. Calculated vapor pressures of dominant species over Cr_2O_3. Data is from reference [34, 44, and 45]
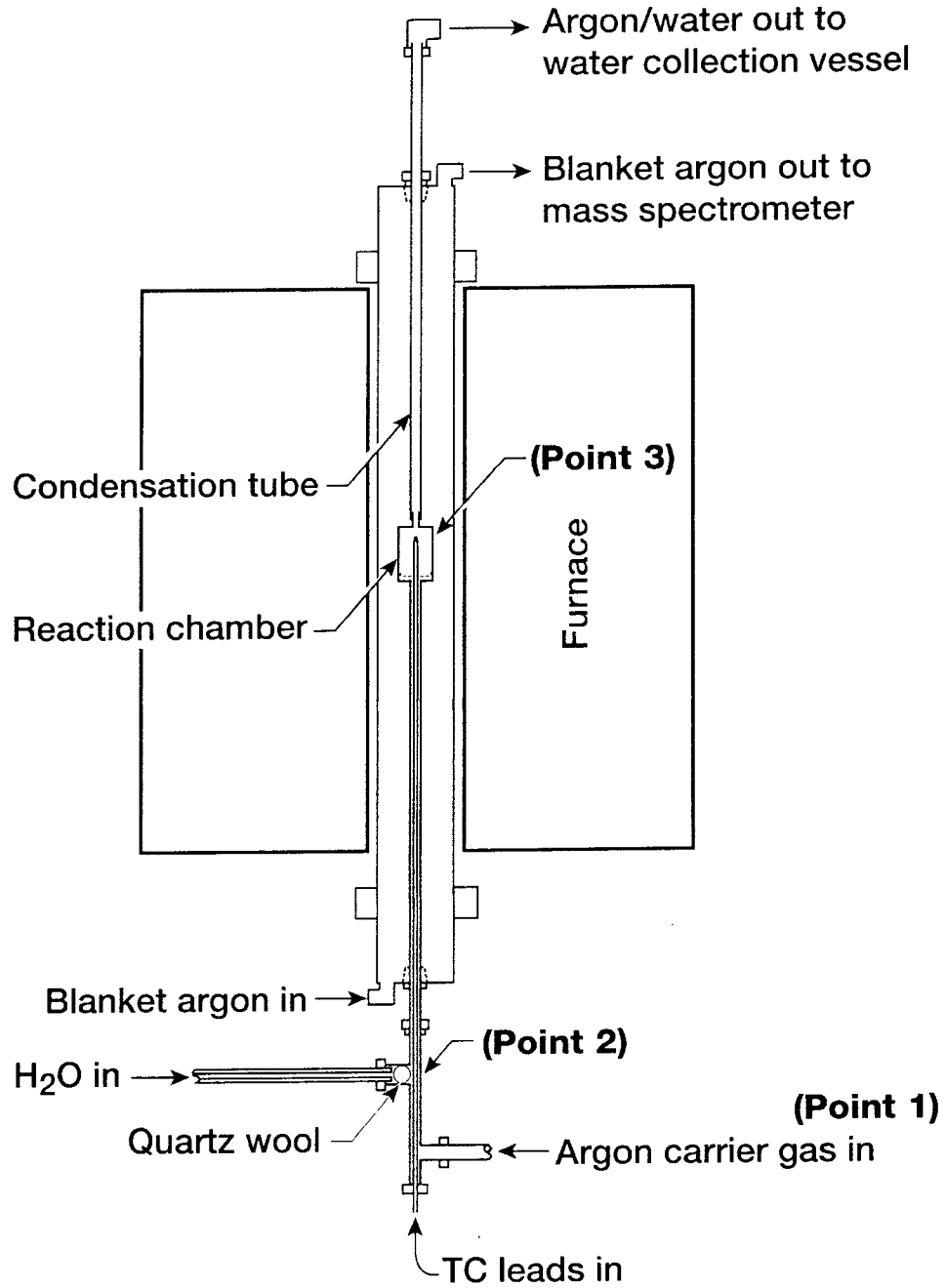
Figure 2. Schematic of our transpiration system.

CD-03-82425
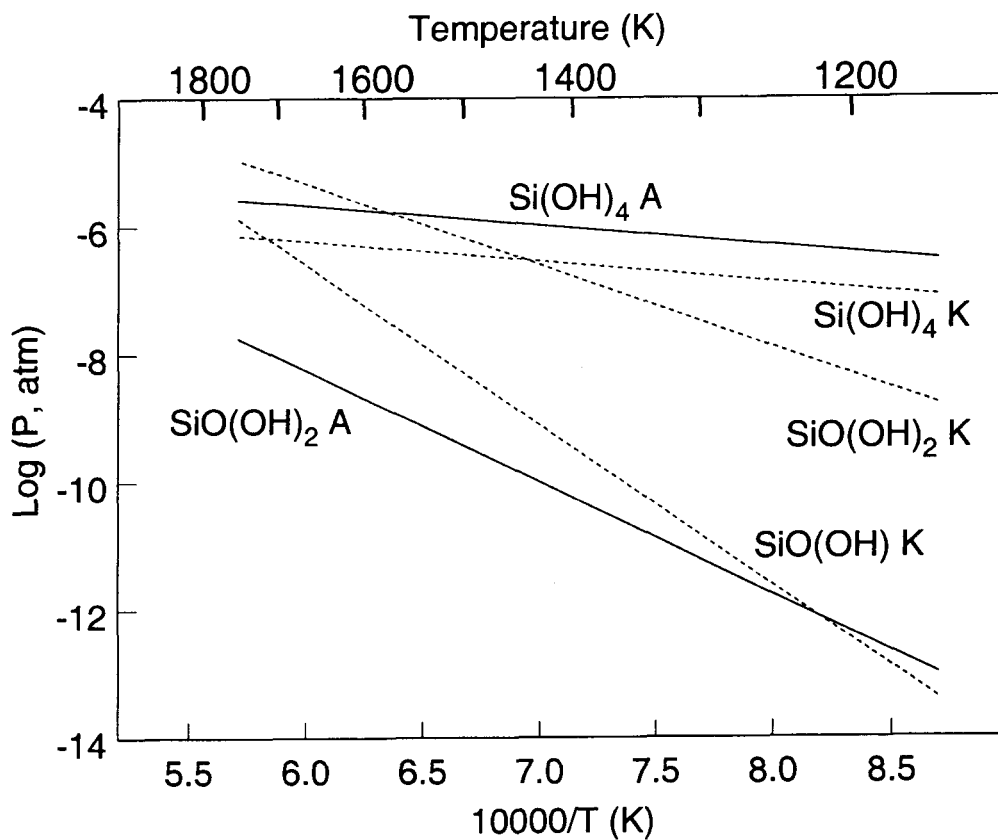
Figure 3. Calculated vapor pressure of Si-OH species over SiO_2 with $x(H_2O)$ = 0.37 and P(total) = 1 bar. The lines labeled K were calculated from thermodynamic functions taken from Krikorian's estimates based on the pseudo halide behavior of the hydroxyl group. The lines labeled A were calculated from the thermodynamic functions taken from Allendorf's *ab initio* calculations.
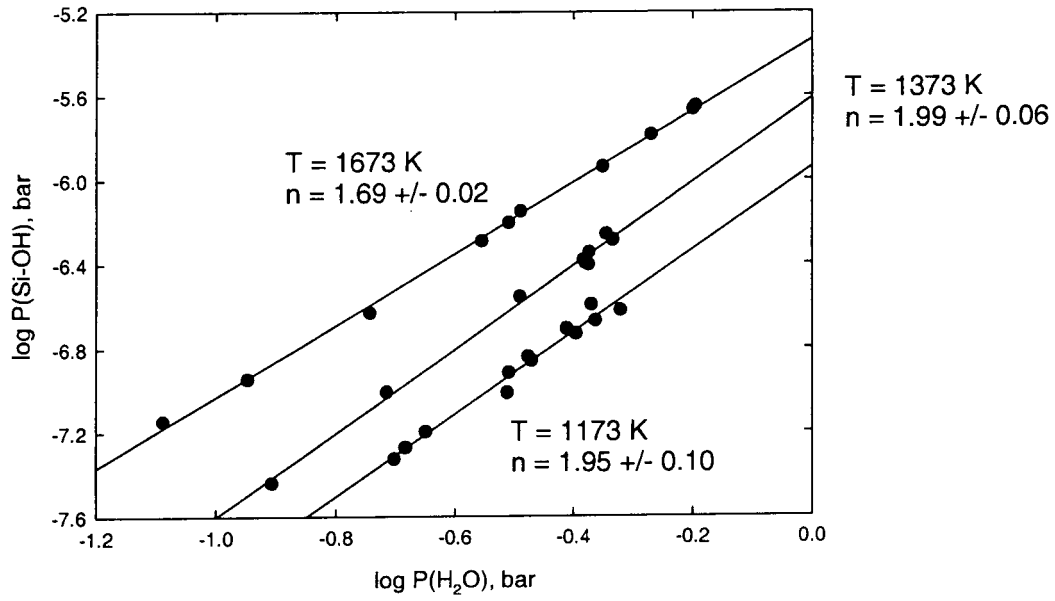
Figure 4. Pressure dependence of Si-OH formation.
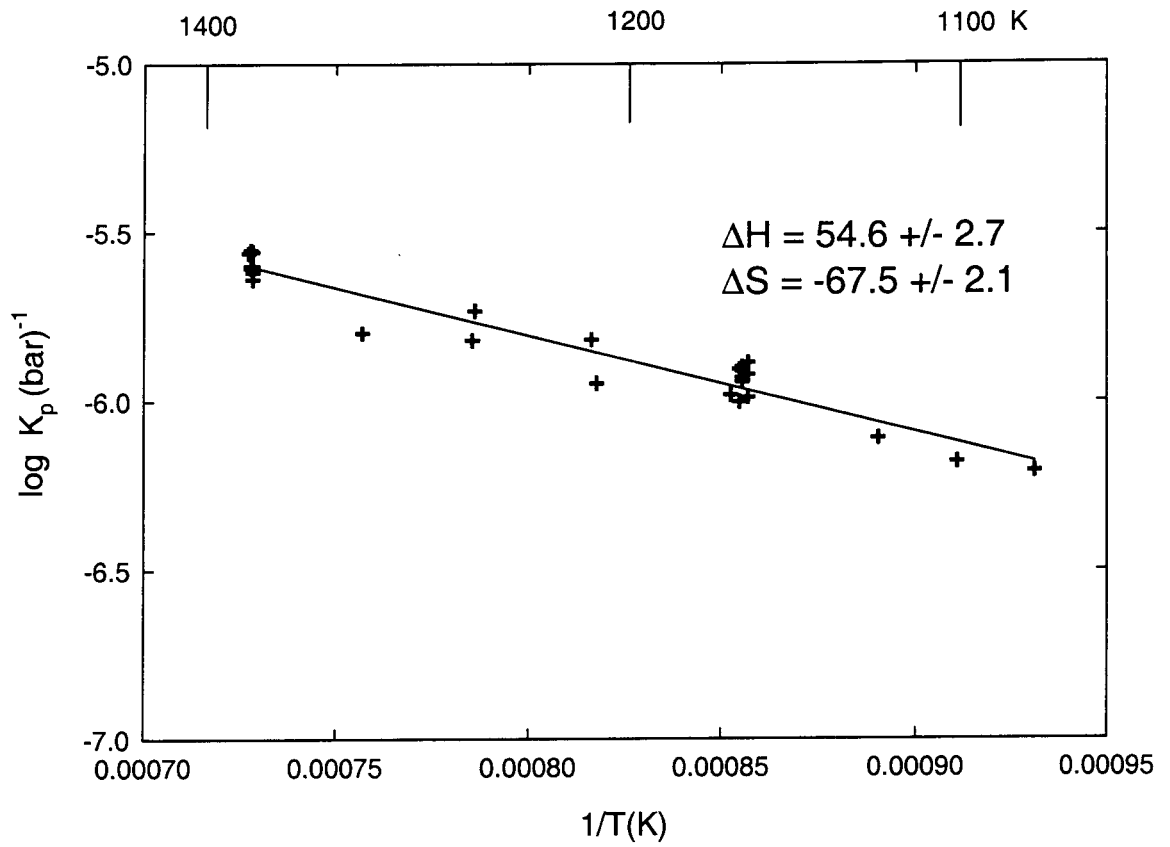
Figure 5. Plot of ln K_p vs 1/T for $SiO_2(s)$ + 2 $H_2O(g)$ = $Si(OH)_4(g)$.